Acta Cryst. (1996). B52, 479–486

Anomalous Dispersion Analyses of the Ni-Atom Site in an Aluminophosphate Test Crystal Including the Use of Tuned Synchrotron Radiation

M. HELLIWELL,[a]* J. R. HELLIWELL,[a] A. CASSETTA,[a]† J. C. HANSON,[b] T. ERICSSON,[c]‡ A. KRICK,[c] V. KAUČIČ[d] AND C. FRAMPTON[e]

[a]*Department of Chemistry, University of Manchester, Manchester M13 9PL, England,* [b]*Chemistry Department, Brookhaven National Laboratory, Upton, NY 11973, USA,* [c]*ESRF, BP220 Grenoble, France,* [d]*National Institute of Chemistry and National University of Ljubljana, 61000 Ljubljana, Slovenia, and* [e]*Roche Products, Welwyn Garden City, Herts, England*

(Received 7 December 1995; accepted 11 January 1996)

Abstract

Data were collected close to the Ni K edge, using synchrotron radiation at the National Synchrotron Light Source, and using a Mo $K\alpha$ rotating anode, from a crystal of a nickel-containing aluminophosphate, $NiAl_3P_4O_{18}C_4H_{21}N_4$ (NiAPO). These data sets, along with an existing Cu $K\alpha$ rotating anode data set, allowed the calculation of several f' difference-Fourier maps exploiting the difference in f' for Ni between the various wavelengths. These differences are expected to be 7.8, 4.5 and 3.3 e for Mo $K\alpha$ data to SR (synchrotron radiation), Cu $K\alpha$ to SR and Mo $K\alpha$ to Cu $K\alpha$, respectively. The phases were calculated either excluding the Ni atom or with Al at the Ni-atom site. The f' difference-Fourier maps revealed peaks at the Ni-atom site, whose height and distance from the refined Ni-atom position depended on the f' difference and the phase set used. The largest peak was located at a distance of only 0.025 Å from the refined Ni-atom site and was obtained from the f' difference map calculated with the coefficients $|F_{\text{Mo }K\alpha} - F_{\text{SR}}|$, using phases calculated with Al at the Ni-atom site. In all cases, it was found that these phases gave optimal results without introducing bias into the maps. The results confirm and expand upon earlier results [Helliwell, Gallois, Kariuki, Kaučič & Helliwell (1993), *Acta Cryst.* B**49**, 420–428]. The techniques described are generally applicable to other systems containing anomalous scatterers in chemical crystallography.

1. Introduction

Microporous materials such as aluminophosphates have found increasing importance in recent times, due to their activity as solid acid catalysts. They tend to be more selective and they avoid the use of environmentally harmful reagents required in the old processes. Incorporation of metallic elements into the neutral aluminophosphate framework places a negative charge on the framework, which gives rise to possible catalytic activity. To understand the role of the incorporated metal atoms it is vital to pinpoint their position within the aluminophosphate framework. Normally, incorporation by the metal atom takes place at one (or more) of the aluminium sites in the framework. This usually leads to partial occupancy of the metal atoms in these positions, sometimes to a degree of only a few per cent. To determine the site of incorporation is a challenging problem for the crystallographer, particularly since the crystals are normally very small and weakly diffracting (see Helliwell, Gallois, Kariuki, Kaučič & Helliwell, 1993).

The problem has been addressed in several recent papers. In Cheetham, Harding, Rizkallah, Kaučič & Rajić (1991), the site of incorporation of Co in CoAPO-21 was determined using data obtained with synchrotron radiation and the FAST detector, on station 9.6 at Daresbury, by refinement of the occupancy. In Helliwell *et al.* (1993), the site of Cr incorporation in CrAPO-14 was determined from the lowering of the temperature factor at the Al position where incorporation occurred, which allowed a value for the percentage occupancy by Cr at that site to be calculated. Recently, we demonstrated that the site of incorporation of Ni in NiAPO could be determined from an f' difference map, using data sets collected at Cu $K\alpha$ and Mo $K\alpha$ wavelengths (*i.e.* using conventional X-ray sources) and phases calculated excluding the Ni atom (Helliwell, Gallois, Kariuki, Kaučič & Helliwell, 1993). In the latter study the Mo $K\alpha$ data set was rather weak since it was collected using a sealed-tube source and the crystal was very weakly diffracting. Nevertheless, a peak of six times the r.m.s. value was obtained 0.8 Å from the Ni-atom site. In the study reported here the Mo $K\alpha$ data set was improved considerably by data collection using a rotating anode rather than a sealed tube source. Also, phases were produced in two ways, the first by removing the Ni atom from the refinement (as in Helliwell, Gallois, Kariuki, Kaučič & Helliwell, 1993), the second by refinement of the model with aluminium incorporated at the Ni-atom site. The latter phase set

† Present address: ELETTRA, Trieste, Italy.
‡ Present address: Chalmers University of Technology and University of Göteborg, S-41296 Göteborg, Sweden.

led to improvements in the size of the peak heights as well as their positions. Clearly, the signal can also be enhanced by the use of synchrotron radiation, tuning close to the Ni K edge in order to optimize the difference in f' for nickel. In this paper, we report on the use of the improved Mo $K\alpha$ data and strategies as well as a synchrotron radiation data collection very close to the Ni K edge. The determination of the Ni-atom site for NiAPO is confirmed, but with an enhanced peak height and considerable improvement in coordinate accuracy.

The results presented here provide a test for developing element-specific wavelength-variable techniques to pinpoint anomalous scatterers. The methods used are of general interest in applications of SR to chemical crystallography and structural science (Coppens, 1992; Helliwell, 1992; Hendrickson, 1991), but, in particular, the results and conclusions drawn are applicable to aluminophosphate and other microporous samples. In this example, enhancing the peak heights by using SR for data collection at the f' dip of the anomalous scatterer, as well as the much increased intensity, allows minor sites of nickel incorporation to be investigated. For other samples, in which the transition metals are incorporated at aluminium sites in low concentration, enhancement of peak heights by the use of SR should permit such sites to be located. Finally, some samples contain more than one anomalous scatterer and for these it would be essential to use SR to locate and identify the elements incorporated at particular sites by data collection at the absorption edge for each element in turn.

2. Experimental

Data were collected at three wavelengths, using the same crystal in all cases. The order of data collections was Cu $K\alpha$ rotating anode, Mo $K\alpha$ sealed-tube, Mo $K\alpha$ rotating anode and synchrotron radiation data from the NSLS (National Synchrotron Light Source). Previously, Helliwell, Gallois, Kariuki, Kaučič & Helliwell (1993), reported on the collection and use of the first two data sets. Here, we report details of the additional data collections, Table 1 summarizes the experimental parameters for all four data sets.

2.1. *Mo $K\alpha$ rotating anode data*

The Mo $K\alpha$ data were collected using a 12 kW rotating anode source and a Rigaku AFC-7*R* diffractometer at Roche Products Ltd, by standard methods similar to those employed in the collection of the Cu $K\alpha$ data set (Helliwell, Gallois, Kariuki, Kaučič & Helliwell, 1993). Data were collected to a maximum 2θ of 54.2° ($0 < h < 12$, $0 < k < 20$, $-18 < l < 17$). The intensities of three standards measured every 150 reflections showed no signs of decay. Structure refinement (*SHELXL*93: Sheldrick, 1992) was carried out using the model obtained from the Cu $K\alpha$ data. All non-H atoms were refined anisotropically. H atoms attached to nitrogen and carbon were placed in calculated positions using the riding model, with isotropic temperature factors 1.2 times that of the atom to which they were bonded. H atoms of the water molecules could not be located. The original Mo $K\alpha$ data set had been collected using a sealed-tube source and an AFC-6*S* diffractometer (Helliwell, Gallois, Kariuki, Kaučič & Helliwell, 1993). Table 1 shows that the use of a rotating anode Mo $K\alpha$ source, rather than a sealed-tube source, has considerably increased the number of observed data, allowing all non-H atoms to be refined anisotropically with the data-to-parameter ratio 8.70.

2.2. *NSLS data collection*

Data collection was carried out at the NSLS on beam-line X7B (Gmr, 1993). This beamline comprises a tuneable double crystal monochromator, followed by a horizontally focusing mirror, designed by Hastings, Suortti, Thomlinson, Kvick & Koetzle (1983). These optics allow a beam intensity of 1% homogeneity over an area of $0.3 \times 0.3\,mm^2$ to be produced at the sample position, which is 22 m from the source. In two directions of the NiAPO crystal the crystal size is much smaller than this area, although the needle length of 0.25 mm is a good match. However, there is movement of the beam position of more than 0.5 mm during a beam fill and consequently the beam could move off the sample over the period of the fill (approximately 15 h). In order to keep the beam on the sample, the diffractometer (a four-circle Huber diffractometer with single counter scintillation detector) was translated in two directions perpendicular to the beam, approximately every 4 h, in a way which maximized the intensity on the ion chamber just before the crystal. Standards collected before and after this adjustment showed changes of as much as 25%. The effect of beam movement between diffractometer optimizations was corrected using two standards, which were collected at the beginning, middle and end of these periods.

The K edge of Ni^{II} in NiAPO was determined *via* measurement of the transmission spectrum from a powder sample. A small shift in the edge position to $\lambda = 1.4856$ Å was seen with respect to the Ni K edge in nickel foil ($\lambda = 1.4878$ Å), *i.e.* 12 eV (Fig. 1*a*). This is larger than the expected value for valence state (II) of approximately 5 eV. The spectral bandpass used on the station was 2×10^{-4} (1.7 eV). The stability of the wavelength at this value throughout the crystallographic data collection was monitored approximately every 4 h. An energy scan of the Ni K edge of nickel foil was carried out and the minimum of the derivative of the edge scan was used to check the stability of the monochromator. In a previous trial data collection wavelength instability was a problem, probably due to source or focal spot movements. In the final data collection, however, the variation in the wavelength

Table 1. *Experimental details*

Crystal data				
Chemical formula	$NiAl_3P_4O_{18}C_4H_{21}N_4$	$NiAl_3P_4O_{18}C_4H_{21}N_4$	$NiAl_3P_4O_{18}C_4H_{21}N_4$	$NiAl_3P_4O_{18}C_4H_{21}N_4$
Chemical formula weight	676.77	676.77	676.77	676.77
Cell setting	Monoclinic	Monoclinic	Monoclinic	Monoclinic
Space group	$P2_1/n$	$P2_1/n$	$P2_1/n$	$P2_1/n$
a (Å)	10.005 (10)	10.0209 (8)	10.009 (1)	10.03 (2)
b (Å)	15.843 (17)	15.661 (1)	15.726 (5)	15.67 (2)
c (Å)	14.196 (13)	14.0914 (8)	14.127 (1)	14.14 (2)
β (°)	101.80 (2)	101.216 (5)	101.339 (8)	101.3 (1)
V (Å^3)	2203 (4)	2169.3 (5)	2180.1 (8)	2180 (5)
Z	4	4	4	4
D_x (Mg m^{-3})	2.04	2.07	2.06	2.06
Radiation type	Synchrotron	Cu $K\alpha$ rotating anode	Mo $K\alpha$ rotating anode	Mo $K\alpha$ sealed tube
Wavelength (Å)	1.4863	1.54178	0.71069	0.71069
No. of reflections for cell parameters	29	25	25	10
θ range (°)	10.25–28.6	37.75–39.85	7.25–14.85	4.85–7.4
ω-scan peak width at half height	–	0.35	0.22	0.34
μ (mm^{-1})	5.948	6.213	1.405	1.391
Temperature (K)	295	295	295	296
Crystal form	Needle	Needle	Needle	Needle
Crystal size (mm)	0.25 × 0.05× 0.02	0.25 × 0.05× 0.02	0.25 × 0.05× 0.02	0.25 × 0.05× 0.02
Crystal color	Blue	Blue	Blue	Blue
Data collection				
Diffractometer	Huber	AFC-5*R*	AFC-7*R*	AFC-6*S*
Data collection method	ω–2θ	ω–2θ	ω–2θ	ω–2θ
Scan rate in ω (° min^{-1})	–	4/8	8	2
No. of rescans	0	2	4	3
Scan width (°)	0.8–1.5	0.94 + 0.30tan θ	0.73 + 0.35tan θ	0.73 + 0.30tan θ
Absorption correction	Integration	Empirical	Empirical	Empirical
T_{min}	0.498	0.78	0.91	0.84
T_{max}	0.908	1.00	0.99	1.00
No. of measured reflections	2121	4840	5033	4238
No. of independent reflections	1596	4601	4745	3997
No. of observed reflections	1452	3497	2681	1057
Criterion for observed reflections	$I > 2\sigma(I)$	$I > 3\sigma(I)$	$I > 2\sigma(I)$	$I > 3\sigma(I)$
R_{int}	0.090	0.044	0.092	0.195
θ_{max} (°)	42.5	80.05	27.1	25.05
d_{min} (Å)	1.1	0.78	0.78	0.84
Range of h, k, l	$0 \rightarrow h \rightarrow 9$ $0 \rightarrow k \rightarrow 14$ $-12 \rightarrow l \rightarrow 12$	$0 \rightarrow h \rightarrow 11$ $0 \rightarrow k \rightarrow 18$ $-16 \rightarrow l \rightarrow 16$	$0 \rightarrow h \rightarrow 12$ $0 \rightarrow k \rightarrow 20$ $-18 \rightarrow l \rightarrow 17$	$0 \rightarrow h \rightarrow 12$ $0 \rightarrow k \rightarrow 19$ $-17 \rightarrow l \rightarrow 17$
No. of standard reflections	2	3	3	3
Frequency of standard reflections	120	150	150	150
Intensity decay (%)	See text	None	None	None
Refinement				
Refinement on	F^2	F	F^2	F
R	0.152	0.057	0.0672	0.05
wR	0.441	0.081	0.172	0.055
S	1.116	2.49	1.139	1.17
No. of reflections used in refinement	1452	3497	2681	1057
No. of parameters used	138	309	308	177
H-atom treatment	H atoms included from difference map or placed in calculated positions	H atoms included from difference map or placed in calculated positions	H atoms bonded to N or C atoms placed in calculated positions and refined using a riding model with U_{iso} = $1.2U_{eq}$ of atom to which they are bonded; H atoms in water molecules not located	H atoms included from difference map or placed in calculated positions
Weighting scheme	$w = 4F_o^2/\sigma^2(F_o^2)$	$w = 4F_o^2/\sigma^2(F_o^2)$	$w = 4F_o^2/\sigma^2(F_o^2)$	$w = 4F_o^2/\sigma^2(F_o^2)$
$(\Delta/\sigma)_{max}$	0.002	0.04	0.00	0.00
$\Delta\rho_{max}$ (e Å^{-3})	1.147	0.86	0.84	0.51
$\Delta\rho_{min}$ (e Å^{-3})	−0.821	−0.88	−0.96	−0.54
Extinction method	None	Secondary	None	None
Extinction coefficient	–	0.62793×10^{-6}	–	–
Source of atomic scattering factors	*International Tables for Crystallography* (1992, Vol. C, Tables 4.2.6.8 and 6.1.1.4)	*International Tables for X-ray Crystallography* (1974, Vol. IV, Table 2.3.1)	*International Tables for Crystallography* (1992, Vol. C, Tables 4.2.6.8 and 6.1.1.4)	*International Tables for X-ray Crystallography* (1974, Vol. IV, Table 2.3.1)

was found to be less than 0.0002 Å. Nevertheless, in order to reduce the impact of any wavelength change, the operational wavelength position for crystallographic data collection was in fact set to 1.4863 Å, 0.0007 Å (3.9 eV) removed from the f' dip position. Fig. 1(*b*) shows the plot for f' in the vicinity of the edge as calculated for the free atom (Sasaki, 1989). Since the wavelength was set on the long-wavelength (low-energy) side of the edge, there were no complications from the XANES (X-ray absorption near-edge structure) or EXAFS (extended X-ray absorption fine structure) variations on f'. Hence, assuming that we can obtain the value of f' by shifting by 0.0007 Å to the long wavelength side of the f' dip for the free Ni atom, the calculated value for f' for Ni in NiAPO at 1.4863 Å is −7.6 e.

It was necessary to update the orientation matrix several times during the data collection. The unit-cell volume increased by 1.5% during the experiment, with the major increases in the *b* and *c* cell axes and a small decrease in the *a* axis. The initial values were a = 10.016 (3), b = 15.706 (7), c = 14.131 (2) Å, β = 101.34 (2)°, V = 2179 (2) Å^3, with final cell dimensions a = 9.999 (9), b = 15.865 (16), c = 14.202 (12) Å, β = 101.98 (2)°, V = 2203 (6) Å^3. The bulk of the data collection was carried out using the cell a = 10.005 (10), b = 15.843 (17), c = 14.196 (13) Å, β = 101.80 (2)°, V = 2203 (4) Å^3.

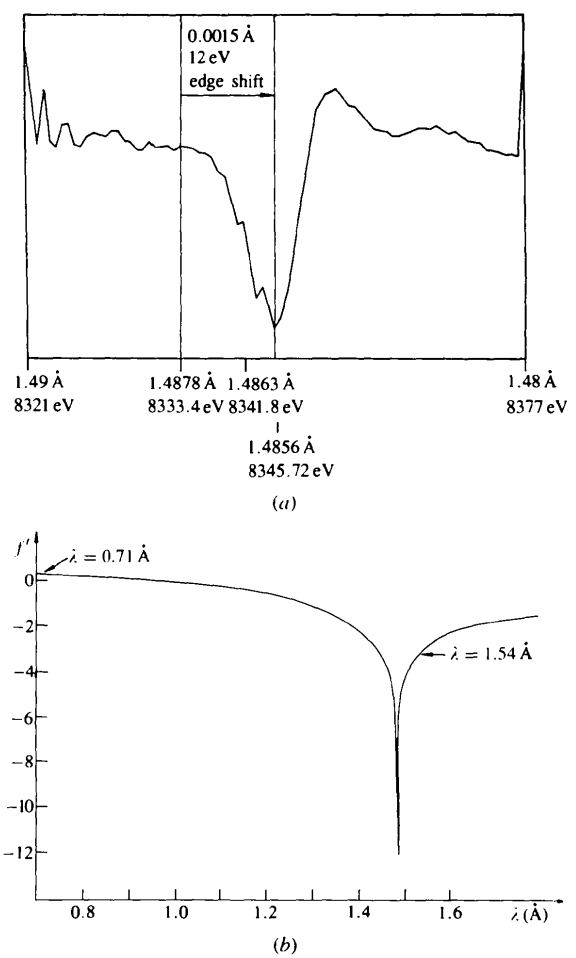

Fig. 1. Variation of f' for the Ni K edge. (*a*) Derivative of the absorption spectrum for NiAPO powder measured at the NSLS. The position of the edge for the free atom and data collection wavelength are indicated. (*b*) Theoretical values for the free atom (Sasaki, 1989); positions for data collection and Mo $K\alpha$ and Cu $K\alpha$ wavelengths are shown.

The data were collected (see Table 1) in a fixed time, step scan mode with the diffracted counts measured with a scintillation counter and the monitor counts collected with a small ion chamber just before the crystal. Time-dependent scale factors were determined using the program *SCALE*3 (Blessing, 1987) based on two standards measured at approximately 2 h intervals. The corrections over 4 h were as high as 25% and account for beam movement relative to the sample, as mentioned before. The data were sorted and merged using the *SORTAV* program (Blessing, 1987). The merging R factors for this data were R_1 = 0.09, R_2 = 0.12, wR = 0.29, with 9 reflections rejected. The absorption correction to the reflection data was performed by Gaussian integration. The total data set to 1.1 Å resolution, measured over *ca.* 1 week, comprised 1596 unique reflections with 1452 reflections having $I > 2\sigma(I)$.

3. Scaling the data sets

Data scaling on F in orthogonal directions of reciprocal space (*i.e.* anisotropic scaling) was carried out using the program *SCALEIT*, which is part of the *CCP*4 program suite (Collaborative Computational Project, Number 4, 1994). Scaling was carried out to produce overall ratios of the mean values of $F^2_{\lambda 1}$ to $F^2_{\lambda 2}$, which were close to unity, and to minimize the overall R and weighted R factors. Results for the *SCALEIT* runs are shown in Table 2.

Optimal results for the scaling of the Cu $K\alpha$ and the Mo $K\alpha$ rotating anode data sets were obtained by employing unit weights and using data with $F > 3\sigma(F)$ for scaling. The (mean $F_{\text{Mo }K\alpha})^2$/(mean $F_{\text{Cu }K\alpha})^2$ plotted *versus* h, k or l showed a smooth and flat variation, and it was only the very weak data that gave ratios which were not close to unity. The weak data also caused the R factor to be 0.164, whilst wR was considerably lower at 0.111.

For the scaling of the SR data to the Mo $K\alpha$ rotating anode data, unit weights were found to give the best results. In addition, reflections with $F < 6\sigma(F)$ in either data set and the low-resolution data below 3.5 Å were removed for the scale determination, but were subsequently scaled and written to the output file. Scaling of the SR data to the Cu $K\alpha$ data was carried out using unit weights and only reflections with $F > 4\sigma(F)$ were used in the scale determination. Although

Table 2. *Summary of the scaling of one data set to another (i.e. SCALEIT runs)*

Data sets and scaling condition	Final scale: (mean $F_{\lambda 1}$)^2/(mean $F_{\lambda 2}$)^2	R factor	Weighted R factor
SR to Mo $K\alpha$ Unit weights Exclude $F < 6\sigma(F)$ and resolution < 3.5 Å	1.003	0.367	0.199
SR to Cu $K\alpha$ Unit weights Excluded $F < 4\sigma(F)$	1.004	0.319	0.363
Cu $K\alpha$ to Mo $K\alpha$ Unit weights Exclude $F < 3\sigma(F)$	0.986	0.164	0.111
Sealed tube to rotating anode Mo $K\alpha$ data Weights from σ's Exclude $F < 3\sigma(F)$	1.002	0.249	0.066

the scaling of the SR data to either of the rotating anode data sets gave overall ratios of the mean values of $F^2_{\lambda 1}$ to $F^2_{\lambda 2}$, which were close to unity, both R and wR were high. In addition, it was noted that there were some odd fluctuations in the ratio of the mean values of $F^2_{\lambda 1}$ to $F^2_{\lambda 2}$ when they were plotted against h, k or l. These were, respectively, a gradual increase in scale with h, an oscillation against k (± 5%) and a gradual decrease with l.

The two Mo $K\alpha$ data sets were scaled and used as a control, this time using weights derived from the standard deviations and excluding data with $F < 3\sigma(F)$ for the scale determination. In this case the sealed-tube data set was relatively weak, particularly at high angle, and it was the weak data that gave [mean $F_{\text{Mo } K\alpha \text{ (rotating anode)}}$]^2/[mean $F_{\text{Mo } K\alpha \text{ (scaled tube)}}$]^2 values which were not close to unity and caused the R factor to be 0.249, whilst wR was 0.066.

4. f' Difference-Fourier calculations

Since the crystal space group, $P2_1/n$, is centrosymmetric, a difference map calculated using structure-factor amplitudes measured at two different wavelengths and appropriate phases corresponds to only the real $\Delta f'$. This is because f'' is 90° out of phase and therefore effectively subtracted out. Moreover, the difference in f' for Al is very small between each wavelength pair compared with the difference for Ni, so that any peak on the difference-Fourier map should be a result of the $\Delta f'$ value of Ni between the two wavelengths, at that particular site. Each scaled set of data was combined with phases calculated in two different ways. Phase set (1) was obtained by carrying out a refinement excluding the Ni atom and using the Cu $K\alpha$ data set. The non-H atoms were refined isotropically (*SHELXL*93; Sheldrick, 1992) using all 3198 reflections with $2\theta <$ 120°, while H atoms were placed in calculated positions and unit weights were used. Refinement of the 134 parameters gave a final R factor of 0.452. Phase set (2) was computed with Al substituted at the Ni-atom site, the isotropic temperature factor of this Al atom was fixed and other conditions were as before. Refinement of the 137 parameters led to a final R factor of 0.199. The scaled data sets were combined with each phase set and it was then possible to compute f' difference maps using the program *FFT*, from the *CCP*4 program suite (Collaborative Computation Project, Number 4, 1994). The maps were placed on an absolute scale by applying the correct scale factors in *FFT* (obtained from the appropriate *SHELXL*93 refinements).

4.1. $|F_{Mo\,K\alpha} - F_{Cu\,K\alpha}|$

The $\Delta f'$ value for Ni between Mo $K\alpha$ and Cu $K\alpha$ is 3.3 e, whilst $\Delta f'_{Al}$ is –0.15 e (Sasaki, 1989). The f' difference-Fourier maps were calculated, excluding reflections with $F < 4\sigma(F)$ from the Cu $K\alpha$ data and differences greater than 3.69 times the mean difference. Using phase set (1), a peak height of 4.34 (13 times the r.m.s. value) was obtained at a position 0.210 Å away from the final refined Ni-atom position. Phase set (2) led to a peak height of 6.93 (21 times the r.m.s. value), which was 0.189 Å away from the refined Ni-atom site. Previously (Helliwell, Gallois, Kariuki, Kaučič & Helliwell, 1993), using phases essentially identical to phase set (1), and the data scaling program *ANSC*, an f' difference-Fourier map using sealed-tube Mo $K\alpha$ data gave a peak of six times the r.m.s. value, 0.8 Å away from the final refined Ni-atom position.

Since the $\Delta f'_{Ni}$ value between Mo $K\alpha$ and Cu $K\alpha$ wavelengths is known precisely to be 3.3 e, it also was possible to use the peak height obtained in the difference-Fourier map calculated between these two wavelengths as a reference with which to calibrate the other difference-Fourier maps. This allowed the calculation of $\Delta f'_{Ni}$ for the other wavelength pairs directly from the peak heights obtained in corresponding f' difference-Fourier maps. Table 3 summarizes the results obtained using phase set (2).

4.2. $|F_{Mo\,K\alpha} - F_{SR}|$

The $\Delta f'$ value for Ni between the Mo $K\alpha$ and SR wavelengths is approximately estimated as 7.8 e, whilst $\Delta f'_{Al}$ is –0.14 e, using values from Sasaki (1989). The f' difference-Fourier maps were calculated, excluding reflections with $F < 4\sigma(F)$ from the SR data and differences greater than 3.51 times the mean difference. Using phase set (1), a peak of height 10.63 was obtained at a position 0.045 Å away from the final refined Ni-atom position. Thus, if we use as a reference the peak height obtained in the map $|F_{Mo\,K\alpha} - F_{Cu\,K\alpha}|$ and phase set (1), an estimated value for the difference in f' of 8.2 e is obtained. Phase set (2) led to a peak of height

Table 3. *Estimates of $\Delta f'$ values derived from electron-density maps from the different wavelengths, i.e. SR (1.4863 Å), Mo $K\alpha$ and Cu $K\alpha$ using phases obtained by refinement of the model with Al at the Ni-atom site*

Data	Peak	(r.m.s.)	Relative peak height	Estimate* of $\Delta f'$ (e) using the (Mo $K\alpha$–Cu $K\alpha$) value	Expected† values of $\Delta f'$ (e)	Distance from refined Ni-atom position (Å)
Mo $K\alpha$–SR	18.0	(0.7)	2.6	8.6	7.8	0.025
Cu $K\alpha$–SR	13.8	(0.6)	2.0	6.6	4.5	0.057
Mo $K\alpha$–Cu $K\alpha$	6.9	(0.3)	1	—	3.3	0.189
Mo $K\alpha$–Mo $K\alpha$‡	1.2	(0.2)	0.17	0.6	0	—
Cu $K\alpha$§	48.7	(2.3)	7.1	23.3 (f_o+f')	22.9 (f_o+f')	0.036
Mo $K\alpha$§	55.8	(2.4)	8.1	26.7 (f_o+f')	26.3 (f_o+f')	0.033

* This is derived from the relative peak height values in the electron-density maps scaled to the calculated $\Delta f'$ value between Cu $K\alpha$ and Mo $K\alpha$ of 3.3 e. All data sets had been placed on an absolute scale using refined model scale factors from *SHELXL95* (Sheldrick, 1992). † Based on Fig. 1(*b*) (Sasaki, 1989). ‡ One Mo $K\alpha$ set was measured on a rotating anode AFC-7*R* diffractometer and the other Mo $K\alpha$ set on a sealed tube AFC-6*S* diffractometer. The peak obtained is therefore a noise level estimate. § An electron-density map calculated from Cu $K\alpha$ F_{obs} values yielded a peak height (r.m.s.) of 48.7 (2.3). Comparing this with the Mo $K\alpha$–Cu $K\alpha$ peak height of 6.9 and using the calculated $\Delta f'$ values of 3.3 e yields an estimate for the number at electrons at the Ni-atom position of 23.3 e compared with the expected value for Ni^{II} with $f' = -3.1$ e of 22.9 e. Likewise for Mo $K\alpha$.

18.01 removed by 0.025 Å from the refined Ni-atom site, giving an estimated value for the f' difference of 8.6 e.

4.3. $|F_{Cu\ K\alpha} - F_{SR}|$

$\Delta f'_{Ni}$ between Cu $K\alpha$ and SR wavelengths is approximately estimated as 4.5 e, whilst $\Delta f'_{Al}$ is 0.01 e (Sasaki, 1989). The f' difference-Fourier maps were calculated, excluding reflections with $F < 4\sigma(F)$ from the SR and differences greater than 3.58 times the mean difference. Using phase set (1), the peak height was 8.57 at a position 0.078 Å away from the final refined Ni-atom position. This corresponds to an estimated value for $\Delta f'_{Ni}$ of 6.5 e (see §4.1). Phase set (2) led to a peak height of 13.76 at 0.057 Å away from the refined Ni-atom site, giving an estimated value for $\Delta f'_{Ni}$ of 6.6 e.

In this case, and for the maps in §4.1 and 4.2, the only significant peak lay close to the Ni-atom position; all other features were at the noise level and could not be related to any of the aluminium sites. Thus, there was no evidence for minor sites of nickel incorporation.

4.4. $|F_{Mo\ K\alpha\ (rotating\ anode)} - F_{Mo\ K\alpha\ (sealed\ tube)}|$

Two final difference-Fourier maps were calculated as controls, using the difference between structure-factor amplitudes from the rotating anode and sealed-tube Mo $K\alpha$ data sets and excluding reflections with $F < 4\sigma(F)$ from the sealed-tube data and differences greater than 3.55 times the mean difference. The largest peak was 1.21 using phase set (1) and 1.17 using phase set (2), but in neither case was the peak related to the Ni-atom site. Moreover, subsequent peaks were only slightly lower in height, in contrast to the maps calculated where there was a real f' difference for Ni.

4.5. *Mo $K\alpha$ and Cu $K\alpha$ Fourier maps*

Two additional Fourier maps were calculated using the Cu $K\alpha$ and Mo $K\alpha$ rotating anode F_{obs} values and phase set (2). In each case data with $F < 4\sigma(F)$ were excluded. Peak heights of 48.7 and 55.8 were obtained 0.036 and 0.033 Å from the refined Ni-atom site, respectively. These correspond to estimated values for the number of electrons at the Ni-atom site being 22.9 and 26.3 e, respectively.

Results of the Fourier calculations based on phase set (2) are summarized in Table 3.

5. Refinement of the structure using the SR data

Refinement of the structure with the SR data was carried out using *SHELXL93* (Sheldrick, 1992). The scattering factor for nickel was adjusted to take account of changes in f', f'' and μ at the SR wavelength. For other atoms scattering factors at the Cu $K\alpha$ wavelength were used, since these are not significantly different to those at the SR wavelength.

5.1. *Refinement using the SR data prior to scaling*

The atomic coordinates obtained in the Cu $K\alpha$ rotating anode refinement were used as a starting point. Isotropic refinement was carried out to convergence for all the non-H atoms. Unfortunately, it was found that the agreement factors were considerably higher than those obtained using the Cu $K\alpha$ and Mo $K\alpha$ rotating anode data sets (Table 1). The SR data collection had been complicated and the final merging R factor was quite high. In addition, the temperature factors for all the atoms had increased, this effect being particularly marked for the Ni atom. It appeared that some structural change or decomposition to the crystal had occurred, which was also indicated by the change in unit-cell dimensions of *ca* 1.5% during the course of the SR data collection. When the temperature factor for the Ni atom was fixed at the average value for the three Al atoms, and its occupancy refined, a value of 0.638 (9) was obtained. The occupancy for Ni was then fixed at this value and isotropic refinement continued. However, the R values were still high, even after removing 36 reflections with particularly poor agreement between F_o

and F_c. This indicates a problem in refining a model for the structure, which cannot be attributed to a change in wavelength. Large thermal ellipsoids in the vicinity of Ni indicate problems in this region, but a change of guest molecules in the structural voids cannot be ruled out (see §6). Final refinement of the 138 parameters gave $R = 0.152$, using 1452 reflections with $I > 2\sigma(I)$ and $wR_2 = 0.441$. Other experimental parameters are shown in Table 1.

5.2. *Refinement using the SR data after scaling to the Cu Kα data set*

This was performed to find out whether scaling smoothed out some of the systematic errors. Values of the refined Ni occupancy changed very little, to 0.64 (1), but temperature factors were generally lower and R values were reduced. Refinement of the 138 parameters gave $R = 0.144$ using 1452 reflections with $I > 2\sigma(I)$ and $wR_2 = 0.415$.

6. Final check of the crystal structure

A final data set was collected on the same crystal, using the Cu $K\alpha$ rotating anode diffractometer in Manchester, once it was suspected that structural change to the crystal had occurred during the SR data collection. The unit-cell parameters and cell volume had again changed to $a = 10.017(7)$, $b = 15.872(7)$, $c = 14.212(6)$ Å, $\beta = 102.25(5)°$, $V = 2208(2)$ Å^3, giving an overall change of 1.8% in the cell dimensions and indicating that further structural change had occurred since the NSLS experiment. 3416 unique data were collected to $2\theta = 120°$, of which only 1392 had $I > 3\sigma(I)$, a marked decrease compared with the original experiment, when there were 2653 reflections with $I > 3\sigma(I)$ to $2\theta = 120°$. Also, the mosaic spread had increased and the data were of poor quality. Refinement of the structure using the parameters obtained from the original Cu $K\alpha$ data was carried out using *TEXSAN* software as in Helliwell, Gallois, Kariuki, Kaučič & Helliwell (1993). It was observed that the B factors for all the atoms had increased again, this effect being particularly marked for the Ni atom, the atoms of the ethylene diamine ligands and the non-framework O atom. When the occupancy of Ni was refined, an apparent occupancy for nickel(II) of 0.71 was obtained. Adjusting the Ni occupancy to this value, refinement was continued with Ni, Al and P atoms refining anisotropically, and all other non-H atoms refining isotropically. Refinement on F of the 177 parameters, using 1540 reflections with $I > 2\sigma(I)$, gave a final R factor of 0.188, with $wR = 0.205$. These R values are considerably higher than those obtained using the SR data and indicate that further decay of the sample occurred after the SR experiment. We note that, using the original Cu $K\alpha$ rotating anode diffractometer data set, refinement of the occupancy of the Ni atom gave a value of 0.968 (3).

7. Discussion

We have examined the effectiveness of various data set combinations to yield the best anomalous dispersion signal in terms of peak height and positional accuracy. In all cases phase set (2) led to a larger peak in the difference map, which was closer to the refined Ni-atom position, for all wavelength pairs. Moreover, the fact that the control difference map, $|F_{\text{Mo } K\alpha \text{ (rotating anode)}} - F_{\text{Mo } K\alpha \text{ (sealed tube)}}|$, showed no peak which could be related to the Ni-atom position indicates that the use of either phase set did not lead to bias. Also, the advantage of the Mo $K\alpha$ rotating anode data over the Mo $K\alpha$ sealed tube data was shown in the better structure refinement and Fourier maps for the former over the latter. Interestingly, the use of the new scaling program *SCALEIT* (Collaborative Computational Project, Number 4, 1994), instead of *ANSC* (SERC Daresbury Laboratory, 1986) improved the peak height and positional accuracy in the map $|F_{\text{Mo } K\alpha \text{ (scaled tube)}} - F_{\text{Cu } K\alpha}|$.

We have demonstrated that the computation of f' difference-Fourier maps using the different wavelength pairs show peaks whose heights and positions are related to the $\Delta f'_{\text{Ni}}$ values between the two wavelengths. Thus, the peak heights were in the order $|F_{\text{Mo } K\alpha} - F_{\text{SR}}| > |F_{\text{Cu } K\alpha} - F_{\text{SR}}| > |F_{\text{Mo } K\alpha} - F_{\text{Cu } K\alpha}|$, in accordance with the $\Delta f'_{\text{Ni}}$ values (see Table 3). Also, the positions of the peaks were very close to the Ni-atom site obtained from the final refinement using the initial Cu $K\alpha$ data and it was the $|F_{\text{Mo } K\alpha} - F_{\text{SR}}|$ difference map which led to the peak closest to the Ni-atom site, as would be expected for a larger signal. There were no other significant peaks on any of the difference-Fourier maps and, in particular, no features which could be related to any of the aluminium sites, showing that there was no evidence for minor sites of incorporation by nickel. The theoretical percentage occupancy sensitivity is a function of the expected signal which can be induced by a change of wavelength (*i.e.* here for Mo $K\alpha$–SR it would be 14% $\Delta F/F$, for a $\Delta f'$ of 7.8 e in 34 non-H atoms of average atomic scattering factor 9.5 e) *versus* the errors in the data. In the limit for the latter, 1% data accuracy might be expected, thus suggesting that a 10% occupancy level should ultimately be visible.

During the lengthy procedure to obtain the data sets at different wavelengths, some decay to the crystal occurred, apparently during the SR data collection. This was evidenced initially by a change in the unit cell during the SR data collection and by the high R values obtained from structure refinement using the SR data. Finally, a repeat data collection following the NSLS run, using the Cu $K\alpha$ rotating anode source, did reveal some change in state of the crystal (§6). Hence, for a crystal that can show radiation decay it is important that data be compared at several different wavelengths measured rapidly and close together in time, on the same apparatus (see below).

The change in nickel temperature factor through the whole experiment leads to an apparent reduction in occupancy at the Ni-atom site when this site occupancy is refined. Between the early Cu $K\alpha$ and final Cu $K\alpha$ data collections, an apparent reduction in occupancy of the nickel(II) site by 0.26 (*i.e.* 6.0 e) was observed. This apparent change in occupancy (or decrease in order at this site) means that a fraction of the signal in the Mo $K\alpha$–SR and the Cu $K\alpha$–SR difference maps can, therefore, be attributed to this effect, in addition to an f' change. This is evidenced by comparing columns 5 and 6 of Table 3, whereby the two different estimates of $\Delta f'$ show some systematic discrepancy. By including the part of the signal due to the reduction of refined occupancy in the calculations for the expected peak heights gives 7.8 + 6.0 = 13.8 e for the Mo $K\alpha$–SR map and 4.5 + 6.0 = 10.5 e for the Cu $K\alpha$–SR map. These values represent the maximum expected values, since the decay took place during and after the SR experiment, and these expected peak heights have the ratio 1:31. The peak heights actually obtained were 8.6 and 6.6 e, respectively (see Table 3), giving the ratio 1.30, in close agreement with the expected ratio. The fact that the peak heights are lower than expected could be explained by the fact that decay occurred during and after the SR data collection, so that the reduction in occupancy would be expected to average to a value of less than 6.0 e, leading to reduced peak heights.

Future experiments to determine the site of incorporation of anomalous scatterers in other microporous crystals using SR are planned, but using an image plate or CCD area detector rather than a single counter. This will greatly reduce data collection time, thus allowing a two or more wavelength experiment using the same apparatus. Also, it will reduce the chance of errors due to sample decay with time, or any beam or wavelength instabilities. The use of an image plate will also avoid clipping of the peaks, by the counter or slits, that would arise from anisotropic mosaic spread, which was also a feature of this crystal, although the mosaic spread at the time of the SR experiment was not large. Moreover, data collection could be carried out at the f' minimum, since the wavelength should be stable over the much shorter length of time needed with such a device. The effectiveness of the image plate with a crystal of this size has indeed been demonstrated (Snell *et al.*, 1995), as has the CCD (Helliwell, Deacon, Moon, Powell & Cook, 1996).

It is clear from these experiments that we are able to obtain highly significant peaks in the f' difference maps very close to the correct site. This indicates that it should be possible to locate lower concentrations of metal atoms substituted at aluminium sites in aluminophosphates, using SR tuned to a specific absorption edge, as well as the sites of more than one anomalous scatterer, by data collection at the absorption edge for each element in turn. Moreover, when SR is used in conjunction with the improvements in speed of data collection afforded by an area detector, plus data collected at two or more closely spaced wavelengths with the same device, these results should be further enhanced. These techniques offer exciting extensions to other systems containing anomalous scatterers in chemical crystallography.

The work at Brookhaven National Laboratory, NSLS, was supported by contract DE-AC02-76CH00016 with the US Department of Energy by its Division of Chemical Sciences, Office of Basic Energy Sciences. We are grateful to Roche Products Ltd for data collection facilities and to the University of Manchester for general support. E. Lobkovsky at the Department of Chemistry, Cornell University, provided computational help and support, during MH's sabbatical there. K. Moffat and J. V. Smith of the University of Chicago are thanked for valuable discussions.

References

Blessing, R. H. (1987). *Cryst. Rev.* **1**, 3–58.
Cheetham, G. M. T., Harding, M. M., Rizkallah, P. J., Kaučič, V. & Rajić, N. (1991). *Acta Cryst.* C**47**, 1361–1364.
Collaborative Computational Project, Number 4 (1994). *Acta Cryst.* D**50**, 760–763.
Coppens, P. (1992). *Synchrotron Radiation Crystallography*. New York: Academic Press.
Gmr, N. F. (1993). *NSLS Users Manual: Guide to the VUV and X-ray Beamlines*, 5th ed. Informal Report 48724. Brookhaven National Laboratory.
Hastings, J. B., Suortti, P., Thomlinson, W., Kvick, A. & Koetzle, T. F. (1983). *Nucl. Inst. Methods*, **208**, 55–58.
Helliwell, J. R. (1992). *Macromolecular Crystallography with Synchrotron Radiation*. Cambridge University Press.
Helliwell, M., Deacon, A., Moon, K. J., Powell, A. K. & Cook, M. J. (1996). In preparation.
Helliwell, M., Gallois, B., Kariuki, B. M., Kaučič, V. & Helliwell, J. R. (1993). *Acta Cryst.* B**49**, 420–428.
Helliwell, M., Kaučič, V., Cheetham, G. M. T., Harding, M. M., Kariuki, B. M. & Rizkallah, P. J. (1993). *Acta Cryst.* B**49**, 413–420.
Hendrickson, W. (1991). *Science*, **254**, 51–58.
Sasaki, S. (1989). *KEK*. Report 88-14. National Laboratory for High Energy Physics, Tsukuba, Japan.
SERC Daresbury Laboratory (1986). *CCP*4. *A Suite of Programs for Protein Crystallography*. SERC Daresbury Laboratory, Warrington, England.
Sheldrick, G. M. (1992). *SHELXL*93. *Program for Crystal Structure Refinement*. University of Göttingen, Germany.
Snell, E., Habash, J., Helliwell, M., Helliwell, J. R., Raftery, J., Kaučič, V. & Campbell, J. W. (1995). *J. Synchrotron Rad.* **2**, 22–26.